Rational design and synthesis of solution-processable red-emitting Ir(III) complexes for phosphorescent organic light-emitting diodes

Woosum Cho, Taegyun Lee, Yeong-Soon Gal, Sung-Ho Jin & Jae Wook Lee

Published online: 02 May 2018.

Submit your article to this journal

Article views: 4

View related articles

View Crossmark data

Taylor & Francis
Taylor & Francis Group

Check for updates

Rational design and synthesis of solution-processable red-emitting Ir(III) complexes for phosphorescent organic light-emitting diodes

Woosum Cho[a], Taegyun Lee[a], Yeong-Soon Gal[b], Sung-Ho Jin [a], and Jae Wook Lee[c]

[a]Department of Chemistry Education, Graduate Department of Chemical Materials, Institute for Plastic Information and Energy Materials, Pusan National University, Busan, Republic of Korea; [b]Polymer Chemistry Laboratory, College of Engineering, Kyungil University, Gyeongsan, Republic of Korea; [c]Department of Chemistry, Dong-A University, Busan, Republic of Korea

ABSTRACT

Here, we have rationally designed and synthesized multifunctional red-emitting Ir (III) complex, $(TPQ)_2Ir(acac-OXD)$ based on thiophene-phenylquinoline (TPQ) as main ligand and acetyl acetonate-linked functional group (acac-OXD) as ancillary ligands for highly efficient phosphorescent organic light-emitting diodes (PhOLEDs). Synthesized Ir(III) complexes were characterized by ^1H NMR, mass spectroscopy and their absorption, emission and cyclic voltammetry were steadily investigated. The Ir(III) complex have shown high thermal stability, and exhibited deep-red emission with high quantum yield. In particular, $(TPQ)_2Ir(acac-OXD)$ has shown higher quantum yield than $(TPQ)_2Ir(acac)$. When utilized these complex in solution-processable PhOLEDs, they delivered an excellent device performance.

Introduction

In the fluorescent molecules, the molecular transition from excited to ground states has a few strict rules related to quantum-mechanical conditions that must be satisfied. These rules prevent every excited molecule from emitting a photon and returning to ground state. As a result, fluorescent materials used in organic light-emitting diodes (OLEDs) often generate heat instead of light. This phenomenon has been overcome by phosphorescent materials using a heavy metal atom, such as iridium, bonded to the organic materials (typically comprising of carbon, nitrogen and hydrogen) in an individual molecule [1-4]. Thus design and synthesis of new phosphorescent materials are attracting great interest in the OLEDs for flat panel display. Particularly Iridium(III) complexes with nitrogen heterocycles such as phenylpyridine, isoquinoline and phenylquinoline are well known materials which can exhibit high triplet quantum yields due to mixing of the singlet and triplet excited state via spin–orbit coupling [5-7], which further leads to high phosphorescence yields, enhancing the triplet state. The ultimate aim of new material design and synthesis in OLED research, is to achieve high power

---

efficiency and low power consumption when OLED display is used in real time applications such as mobile appliance [8-10].

It is well known that the carbazole and arylamine units containing Ir(III) complexes are good for hole injection and transportation, whereas the oxadiazole, organoboryl, diarylsulfone and triarylphosphine oxide moieties typically serve as promising electron-deficient components. Here, we focus on the conceptual designs of some multifunctional iridium(III) complexes with distinct C^N chelating ligand chromophores, which are carbazole and oxadizole with phenylquinoline as main skeleton. The incorporation of electron donating units on the C^N chelating ligands is another strategy in enhancing the hole-transporting properties of iridium complexes and it can also induce the longer wavelength emission with pure color quality. Two strategies can be adopted to red shift of phosphorescence cyclometalated Ir(III) complexes. The first one is to decrease the energy of the emissive metal-to-ligand, intraligand or ligand-to ligand charge transfer excited states by introducing electron-donating/electron-withdrawing groups to the ligands and by disrupting communication between the ligands. The second way is to decrease the energy of the emissive $\pi-\pi^*$ ligand-centered states by extended conjugation in the ligand. In our previous report thiophene group has been attached to the phenylquinoline moiety of the Ir(III) complexes to develop novel functionalized phosphorescent red emitters with electron transporting (ET) oxadiazole group [11]. Benefiting from their ET ability, the TPQ-Ir(III) phosphorescent emitters can furnish attractive EL efficiencies in homoleptic and heteroleptic red OLEDs. In addition, TPQ ligands bearing electron donating thiophene and electron accepting phenylquinoline groups have been employed major role to get very high EL efficiencies to the concerned PhOLEDs [12]. In this extension, we introduce the electron transporting and hole transporting moiety in thiophene core for the synthesis of Ir(III) heteroleptic complexes.

Experimental section

General Information

All reactions were carried out in an inert and dry environment under anhydrous nitrogen (N_2) which was dried by passing through a column of calcium sulphate. All chemicals and reagents and solvents were purchased from Aldrich Chemical Co. and Alfa Aesar and used without further purification. (TPQ)$_2$Ir(acac) was synthesized using the reported procedures [13]. ^{1}H NMR spectra was recorded on a Varian Mercury plus 300 MHz spectrometer and chemical shifts were recorded in ppm units with CDCl$_3$ as an internal standard. High-resolution mass spectra data were obtained from the Korea Basic Science and Institute Daejeon Center (HR-ESI Mass). The UV-visible and PL spectra were recorded with JASCO V-570 and Hitachi F-4500 spectrophotometers at room temperature (RT). The absorption and emission spectra were measured by 10^{-5} mol/L in chloroform (CF) solution. Thermal analysis was carried out on Mettler Toledo TGA/SDTA 851e, and DSC 822e analyzer under N_2 atmosphere at a heating rate of 10°C/min. Cyclic voltammetry (CV) measurements were performed with a CHI 600C potentiostat (CH Instruments) at a scan rate of 100 mV/s using anhydrous dichloromethane (CH$_2$Cl$_2$) and 0.1 M tetrabutylammonium tetrafluoroborate (TBABF$_4$) as the solvent and electrolyte, respectively, at RT. A platinum disc was used as the working electrode, a platinum wire as the counter electrode, and a Ag/AgCl as the reference electrode. The potentials were referenced to the ferrocene/ferrocenium redox couple (Fc/Fc+). The sublimated grade of 4,4'-cyclohexylidenebis[*N,N*-bis(4-methylphenyl)benzenamine] (TAPC), and 2,6-bis(3-(9*H*-Carbazol-9-yl)phenyl)pyridine (26DCzPPy) were purchased from OSM and used

as the host materials for emitting layer (EML). The sublimated grade of 1,3,5-tri[(3-pytidyl)-phen-3-yl]benzene (TmPyPB) was purchased from OSM and used as electron transport layer (ETL).

Synthesis of 4-methyl-N-(2-oxo-2-phenylethyl)benzamide (1)

A mixture of 4-methylbenzoyl chloride (1.00 g, 6.4 mmol) and NMP (25 mL) was stirred at 0°C, and a solution of benzoyl hydrazide (0.87 g, 6.4 mmol) in 10 mL pyridine was added. The reaction mixture was stirred at 40°C for 4 h, after which the reaction mixture was poured into 200 mL distilled water. The precipitated product of **1** was collected by filtration (1.05 g, 76%). ^{1}H NMR (300 MHz, Acetone-d_6): δ 8.00-7.87 (m, 4H), 7.52-7.48 (m, 3H), 7.32-7.30 (d, 2H), 2.03 (s, 3H).

Synthesis of 2-phenyl-5-tolyl-1,3,4-oxadiazole (2)

A mixture of 4-methyl-N-(2-oxo-2-phenylethyl)benzamide (1.00 g, 4.0 mmol) in 40 mL POCl$_3$ was stirred at 120°C for 7 h. After cooling to RT, the mixture was poured into ice water. The precipitate was collected by filtration and washed twice with de-ionized water to afford a white powder of 2-phenyl-5-tolyl-1,3,4-oxadiazole (0.56 g, 61%). ^{1}H NMR (300 MHz, CDCl$_3$): δ 8.15-8.02 (m, 4H), 7.55-7.53 (m, 3H), 7.35-7.32 (d, 2H), 2.45 (s, 3H).

Synthesis of 2-(4-(bromomethyl)phenyl)-5-phenyl-1,3,4-oxadiazole (3)

2-phenyl-5-tolyl-1,3,4-oxadiazole (3.00 g, 12.70 mmol), N-bromosuccinimide (2.4 g, 13.90 mmol), and benzoyl peroxide (0.3 g, 0.127 mmol) were dissolved in carbon tetrachloride (80 mL). The reaction mixture was heated to react at 85°C for 5 h. After the reaction was completed, the product in solution was collected by filtration and purified by recrystallization from a solution of CF/methanol (4:1) to give a white solid (2.40 g, 60%). ^{1}H NMR (300 MHz, CDCl$_3$): δ 8.16-8.11 (m, 4H), 7.58-7.55 (m, 5H), 4.54 (s, 2H).

Synthesis of 6-(4-(5-phenyl-1,3,4-oxadiazol-2-yl)phenyl)hexane-2,4-dione (4)

Sodium hydride (50% in mineral oil, 48 mg, 2.0 mmol) was washed with THF (10 mL each) three times. Acetyl acetone (150 mg, 1.5 mmol) was added dropwise to a stirred suspension of sodium hydride in 50 mL THF at 0 °C. The resultant mixture was stirred for a further 30 min at 0°C. N-butyllithium (2.5 M in hexane, 0.6 mL, 1.5 mmol) was added dropwise at 0°C and the resultant mixture was stirred for a further 30 min at 0°C. 2-(4-(bromomethyl)phenyl)-5-phenyl-1,3,4-oxadiazole (150 mg, 0.5 mmol) dissolved in 20 mL THF was added dropwise to the stirred solution at 0°C dropwise. The reaction was kept at 0°C for 1 h and a further 1 h at RT, after which it was quenched with aqueous ammonium chloride (10%, 20 mL). Concentrated hydrochloric acid was added to the mixture until pH 1 was reached, and then the aqueous phase was separated and extracted with diethyl ether. The combined organic phases were washed with saturated sodium bicarbonate and dried over anhydrous sodium sulfate. After removal of the solvent, the crude product was purified by silica gel column chromatography with hexane/DCM (6:1 to 2:1) as eluent to give a white solid (66 mg, 42%). ^{1}H NMR (300 MHz, CDCl$_3$): δ 8.15-8.05 (m, 4H), 7.55-7.53 (m, 3H), 7.37-7.35 (d, 2H), 5.47 (s, 1H), 8.16-8.11 (m, 4H), 3.05-3.00 (t, 2H), 2.67-2.62 (t, 2H), 2.04 (s, 3H)
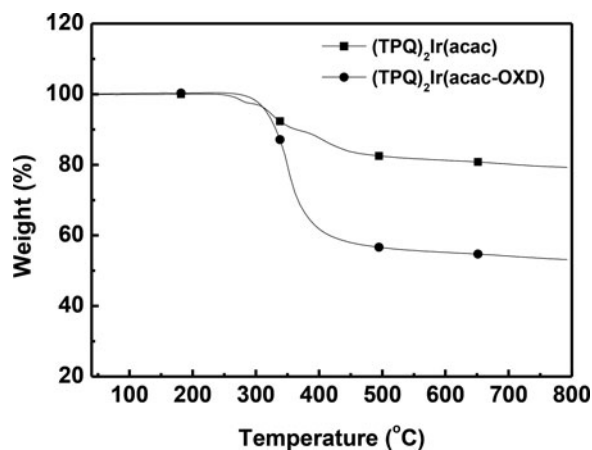
Figure 1. TGA curves of (TPQ)$_2$Ir(acac) and (TPQ)$_2$Ir(acac-OXD) measured at a scan rate of 10 °C/min under N$_2$ atmosphere.

Synthesis of cyclometalated Ir(III) μ-chloride bridged dimer (5)

(4-phenyl-2-(thiophen-2-yl)quinoline) (5 g, 17.40 mmol) and IrCl$_3$·H$_2$O (2.08 g, 6.96 mmol) were added to a mixture of 2-ethoxyethanol and water (80 mL, 3:1 v/v). The resulting mixture was refluxed at 140 °C for 20 h under an N$_2$ atmosphere and cooled to RT. The formed red solid was filtered, washed with water followed by methanol. Subsequently, the solid was dried under vacuum at 120 °C to afford cyclometalated Ir(III) μ-chloride bridged dimer as a red solid (3.36 g, 60%). ^{1}H NMR (300 MHz, CDCl$_3$): δ (ppm) 8.19-8.16 (d, 1H), 8.06-8.05 (dd, 1H), 7.90-7.86 (m, 2H), 7.74-7.69 (m, 2H), 7.56-7.51 (m, 5H), 7.48-7.43 (m, 2H)

Synthesis of bis[4-phenyl-2-(thiophen-2-yl)quinoline]iridium-6-(4-(5-phenyl-1,3,4-oxadiazol-2-yl)phenyl)hexane-2,4-dione (6)

The cyclometalated iridium dimer (280 mg, 0.7 mmol) and 6-(4-(5-phenyl-1,3,4-oxadiazol-2-yl)phenyl)hexane-2,4-dione (150 mg, 0.45 mmol) were mixed with Na$_2$CO$_3$ (47 mg, 0.45 mmol) in 2-ethoxyethanol (50 mL). The mixture was refluxed for 12 h under a N$_2$ atmosphere. After cooling at RT, the crude solution was poured onto water and extracted with ethyl acetate, dried over anhydrous MgSO$_4$ and evaporated in a vacuum. The residue was purified by silica gel chromatography (hexane:ethyl acetate 1:4) as an eluent and further purified by recrystallization twice using dichloromethane/hexane mixture to afford a red solid complex (150 mg, 34%). ^{1}H NMR (300 MHz, CDCl$_3$): δ 8.42-8.38 (m, 2H), 8.10-8.08 (m, 2H), 7.85-7.78 (m, 3H), 7.74-7.72 (d, 3H), 7.66-7.60 (m, 6H), 7.55-7.41 (m, 9H), 7.35-7.30 (m, 3H), 7.21-7.16 (m, 3H), 6.93-6.90 (d, 1H), 6.42-6.36 (d, 1H), 4.84 (s, 1H), 2.57-2.55 (t, 2H), 1.67-1.65 (t, 2H) Calcd for C$_{58}$H$_{41}$IrN$_4$O$_3$S$_2$: C, 62.43; H, 3.76; N, 5.10. Found: C, 62.37; H, 3.74; N, 5.05. HRESI-MS [M+H]$^+$: m/z Found 1098.3265, Calcd for 1098.2240.

Results and discussion

The thermal stability of (TPQ)$_2$Ir(acac-OXD) was identified using a thermogravimetric analyzer (TGA) under N$_2$ atmosphere at a heating rate 10°C/min (Fig. 1). The thermal decomposition temperature (T$_d$) of (TPQ)$_2$Ir(acac-OXD) at 5% mass loss was 316°C. (Fig. 1 and Table 1).

Table 1. Photophysical, electrochemical and thermal properties of (TPQ)$_2$Ir(acac) and (TPQ)$_2$Ir(acac-OXD).

Compound	T$_d$ [°C][a]	λ$_{abs}$ [nm][b]	λ$_{em}$ [nm][c]	HOMO/LUMO [eV][d]
(TPQ)$_2$Ir(acac)	320	296, 361, 436, 488	634	-5.3/-3.4
(TPQ)$_2$Ir(acac-OXD)	316	295, 358, 437, 481	633	-5.4/-3.4

[a]Temperature with 5% mass loss measure by TGA with a heating rate of 10 °C/min under N$_2$.

[b] Absorption maximums in CHCl$_3$ solution at 1.0 × 10^{-5} M concentration.

[c]Maximum emission wavelength, measured in CHCl$_3$ solution at 1.0 × 10^{-5} M.

[d]Determined from the onset of CV for oxidation and UV-visible absorption edge.

The photophysical properties of (TPQ)$_2$Ir(acac-OXD) was measured using UV-visible absorption and PL spectra at RT. The UV-visible absorption spectrum of (TPQ)$_2$Ir(acac-OXD) in CF solution (Fig. 2(a) and Table 1) showed absorption bands at 300–442 nm; these correspond to the spin-allowed $^1\pi$-π^* transitions of the cyclometalated ligands. A well-resolved shoulder at 410 nm confirmed the presence of a spin-forbidden ligand-centered $^3\pi$-π^* transition, facilitated by spin-orbit coupling. A structure-less weak band at 605 nm was assigned to admixture of some ^{1}MLCT and ^{3}MLCT states. The (TPQ)$_2$Ir(acac-OXD) showed a PL emission maximum at 633 nm in CF solution (Fig. 2(b) and Table 1). Due to the presence of donor/acceptor interactions between the electron donor thiophene and
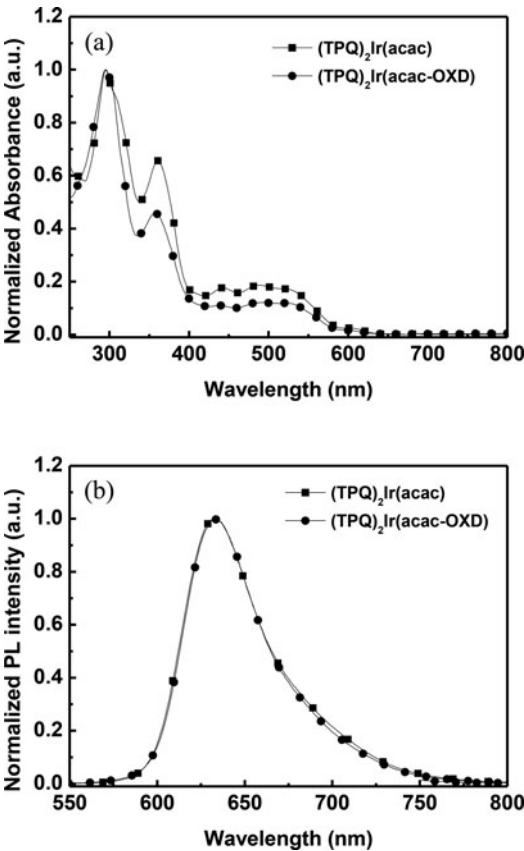

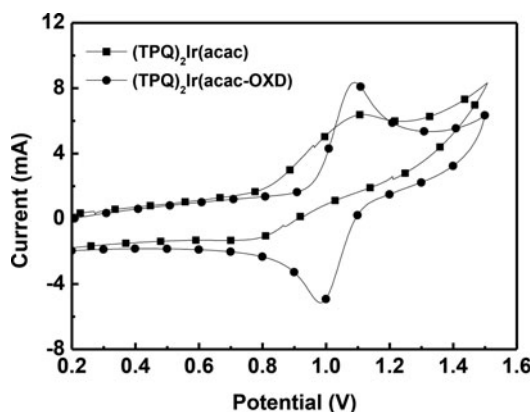**Figure 2.** (a) UV-visible absorption spectra and (b) PL spectra of (TPQ)$_2$Ir(acac) and (TPQ)$_2$Ir(acac-OXD).

Figure 3. Cyclic voltammetry of (TPQ)$_2$Ir(acac) and (TPQ)$_2$Ir(acac-OXD).

electron acceptor quinoline (TPQ) groups in the cyclometalated ligand, the emission maximum of (TPQ)$_2$Ir(acac-OXD) complex was shifted to the bathochromic region. The donor-acceptor character is caused by interaction between electron-rich thiophene and electron-deficient quinoline [12]. CV analysis was carried out for (TPQ)$_2$Ir(acac-OXD) in anhydrous CH$_2$Cl$_2$ solvent with 0.1 M TBAClO$_4$ as supporting electrolyte at a scan rate of 100 m/Vs to find out the highest occupied molecular orbital (HOMO) energy level. The lowest unoccupied molecular orbital (LUMO) energy level was calculated from the HOMO and optical band gap (E$_g^{opt}$), obtained from UV absorption edge value. The experimental HOMO and LUMO energy levels of (TPQ)$_2$Ir(acac-OXD) are -5.43 eV and -3.41 eV, respectively (Fig. 3). Here, E$_g^{opt}$ of (TPQ)$_2$Ir(acac-OXD) is 2.02 eV. Both the HOMO and LUMO levels of (TPQ)$_2$Ir(acac-OXD) are very close to the corresponding energy levels of (TPQ)$_2$Ir(acac) representing that the introduction of either oxadiazole-based ET group on ancillary ligand does not much influence the frontier orbital energy levels of these Ir(III) complexes as similar to the photophysical properties.

Before fabrication of the PhOLEDs with the new dopant, we measured the electron and hole mobilities of the dopant [(TPQ)$_2$Ir(acac-OXD)] by using space-charge limited current (SCLC) [14] method with the device configuration of ITO/ LiF (10 nm)/Ir(III) complex (100 nm)/LiF (1 nm)/Al (100 nm) for electron-only device and ITO/PEDOT:PSS (40 nm)/Ir(III) complex (100 nm)/MoO$_3$ (5 nm)/Al (100 nm) for hole-only device. The electron and hole mobilities of (TPQ)$_2$Ir(acac) and (TPQ)$_2$Ir(acac-OXD) were also measured by the same method (Table 2). The J-V^2 plots for the devices are shown in Fig. 4. The electron and hole mobilities of (TPQ)$_2$Ir(acac-OXD) are found to be 7.75 × 10^{-5} cm^2/V s and 1.63 × 10^{-5} cm^2/V s, respectively. This result clearly shows that tethering of OXD unit to the Ir(III) complex improved the electron mobility as compared with (TPQ)$_2$Ir(acac).

In order to evaluate the performance of (TPQ)$_2$Ir(acac-OXD) as emitter, we fabricated deep-red emitting PhOLEDs with a simple device structure containing a solution-processed EML (Fig. 5). The device configuration adopted in this study is

Table 2. Mobility data for (TPQ)$_2$Ir(acac-OXD) in comparison with (TPQ)$_2$Ir(acac).

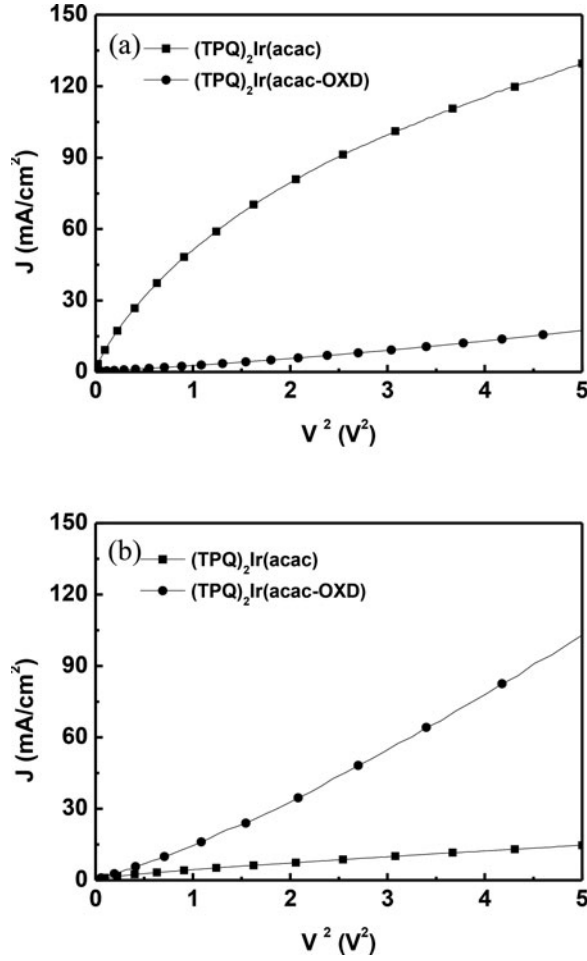| Ir(III) complex	Hole mobility (cm^2/V s)	Electron mobility (cm^2/V s)
(TPQ)$_2$Ir(acac)	6.93 × 10^{-5}	8.56 × 10^{-6}
(TPQ)$_2$Ir(acac-OXD)	1.63 × 10^{-5}	7.75 × 10^{-5}

Figure 4. (a) Hole only device and (b) electron only device of J-V^2 characteristics [ITO/LiF (10 nm)/Ir(III) complex (100 nm)/LiF (1 nm)/Al (100 nm) for electron-only device and ITO/PEDOT:PSS (40 nm)/Ir(III) complex (100 nm)/MoO$_3$ (5 nm)/Al (100 nm) for hole-only device].
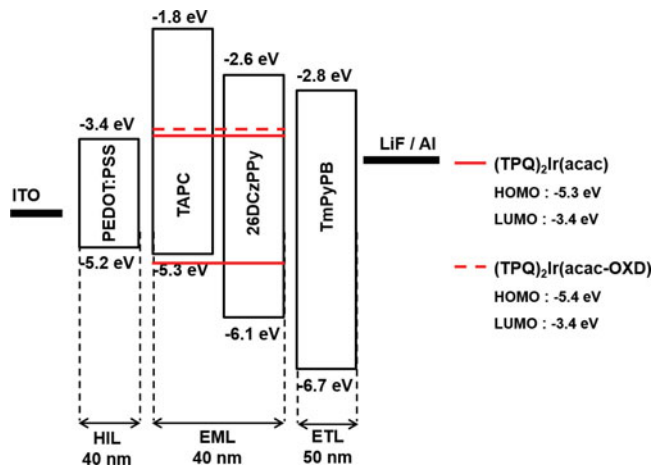

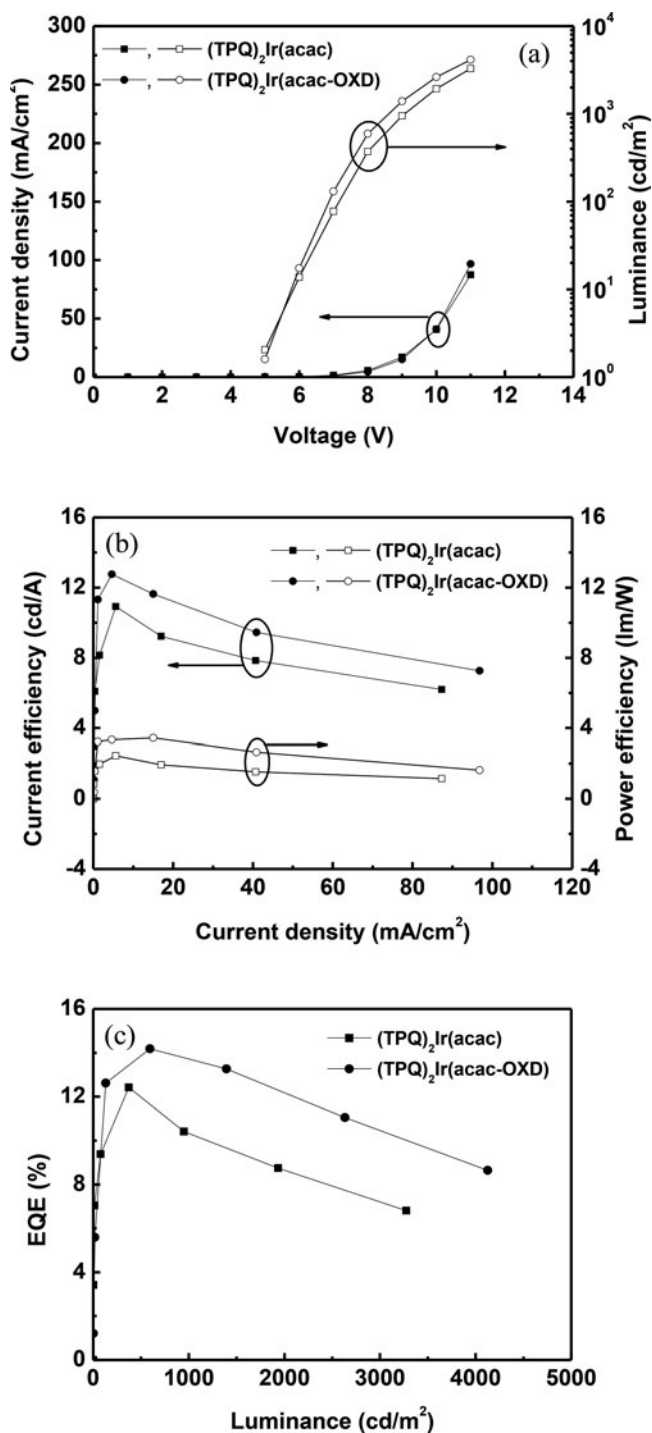**Figure 5.** Energy level diagram of the deep-red PhOLEDs.

Figure 6. Characteristics of the deep-red PhOLEDs using (TPQ)$_2$Ir(acac) and (TPQ)$_2$Ir(acac-OXD) as dopants: (a) J-V-L (b) CE-V-PE and (c) EQE-V.
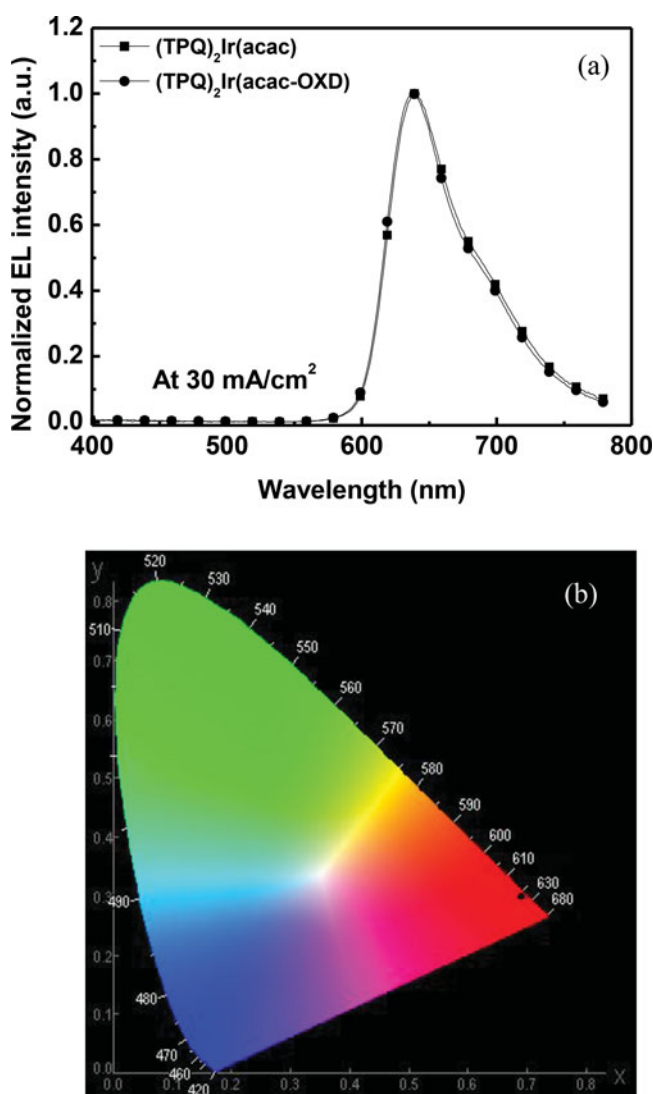
Figure 7. EL spectra of (a) deep-red PhOLEDs and (b) CIE coordinates using (TPQ)$_2$Ir(acac) and (TPQ)$_2$Ir(acac-OXD) as dopants.

ITO/PEDOT:PSS/TAPC:26DCzPPy:12 wt% dopant/TmPyPB/LiF/Al. We have also fabricated the control devices using (TPQ)$_2$Ir(acac) as dopant to compare the effect of OXD group on device performance.

Data of the PhOLEDs are provided in Table 3. Fig. 6(a) & 6 (b) shows the current density-voltage-luminance (J-V-L) and current efficiency-J-power efficiency (CE-J-PE) characteristics. The CE and PE of TPQIr-HT are 12.76 cd/A and 3.44 lm/W, respectively, which are higher than the CE (10.92 cd/A) and PE (2.45 lm/W) of (TPQ)$_2$Ir(acac). The high electron mobility of (TPQ)$_2$Ir(acac-OXD) relative to (TPQ)$_2$Ir(acac) results good charge balance in EML, which enhances the performance of (TPQ)$_2$Ir(acac-OXD) in PhOLEDs.

All the PhOLEDs, irrespective of the dopant, HIL, and luminance range, exhibited the same electroluminescent (EL) peak at 637 nm (Fig. 7(a)) and the CIE coordinates of (0.69, 0.30) (Fig. 7(b)) representing the saturated red/ deep-red emission, which is highly sought-after as
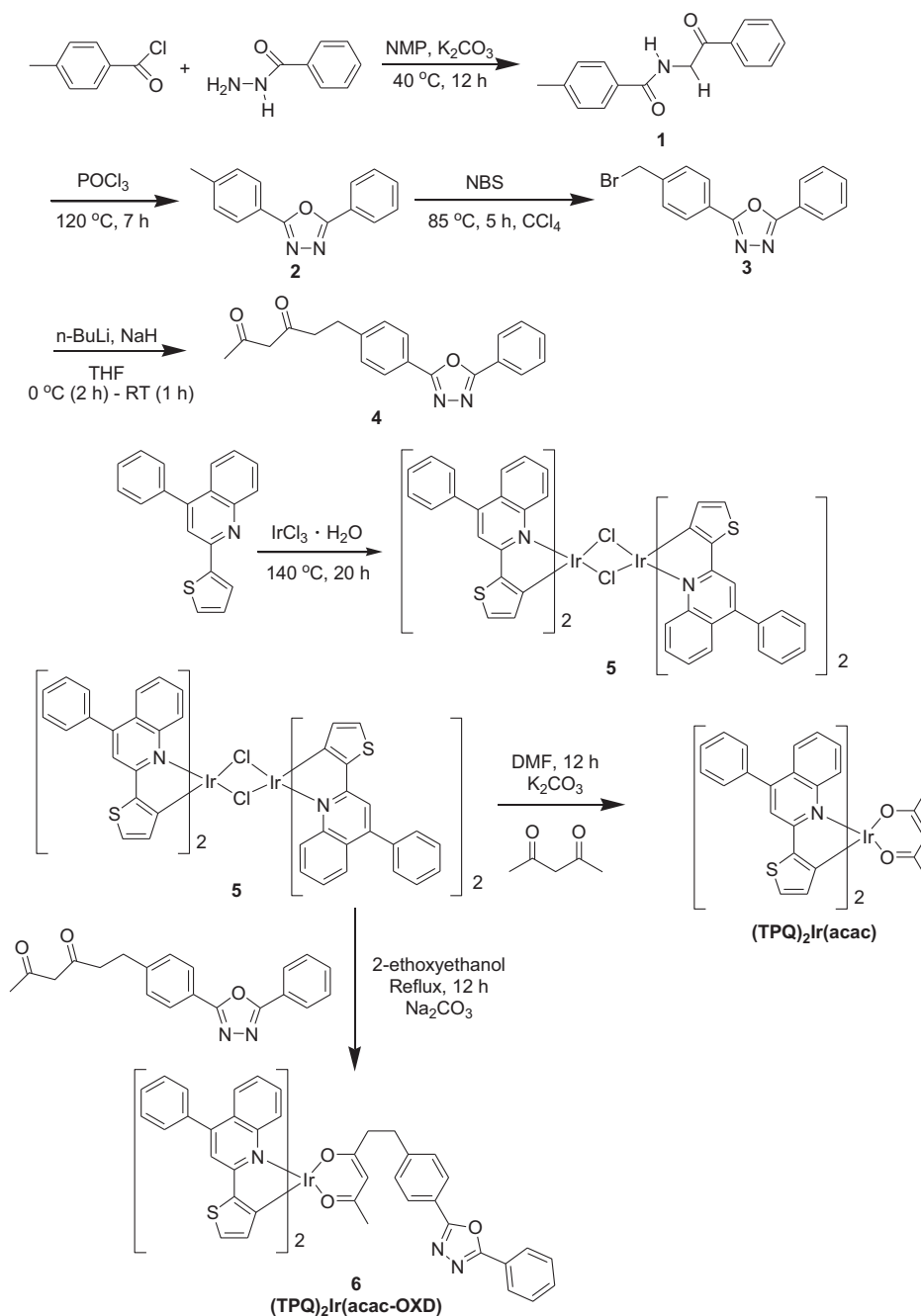
Scheme 1. Synthesis of Ir(III) complexes

like deep-blue emission. The color coordinates and the efficiency of (TPQ)$_2$Ir(acac-OXD) are better than our previously reported solution-processed PhOLEDs containing diphenylquino-line (DPQ) based and carbazole (CVz)-phenylquinoline(PQ) based deep-red emitting het-eroleptic Ir(III) complexes (FPQ)$_2$Ir(pic-N-O) [15], and (EO-CVz-PhQ)$_2$Ir(acac) [16].

Table 3. Device performance of the deep-red PhOLEDs with (TPQ)$_2$Ir(acac) and (TPQ)$_2$Ir(acac-OXD) as dopants.

Compound	V_{on} [V][a]	EQE [%][b]	Luminance [cd/m^2][b]	EL [nm][c]	CIE (x,y)[c]
(TPQ)$_2$Ir(acac)	4.78	12.42	3275	638	(0.694, 0.301)
(TPQ)$_2$Ir(acac-OXD)	4.88	14.18	4127	637	(0.692, 0.302)

[a]Turn-on voltage measured at brightness of 1 cd/m^2.
[b]Maximum efficiency.
[c]At 30 mA/cm^2.

Conclusion

In summary, we attached a oxadizole based ET unit (OXD) to the heteroleptic Ir(III) complex, (TPQ)$_2$Ir(acac), to achieve a good charge balance in EML by improving the electron transporting as well as hole transporting properties of (TPQ)$_2$Ir(acac-OXD) as compared with the parent complex. Upon introduction of OXD moiety, carrier mobilities and the device performance are improved relative to (TPQ)$_2$Ir(acac), without affecting the deep-red coordinates (0.67, 0.32). We achieved a high EQE of 14.18% for the PhOLED of (TPQ)$_2$Ir(acac-OXD), which is superior to the performance of (TPQ)$_2$Ir(acac) (EQE = 12.42%). The overall results of these deep-red PhOLEDs show that the introduction of new functional units is an effective method to improve device performance.

Funding

ORCID

Sung-Ho Jin http://orcid.org/0000-0001-6631-983X

Reference

[1] Uoyama, K., Goushi, K., Shizu, K., Nomura, H. & Adach, C. (2012) *Nature* 492, 234.
[2] Tang, C. W. & VanSlyke, S. A. (1987) *Appl. Phys. Lett.* 51, 913.
[3] Baldo, M. A., O'Brien, D. F., You, Y., Shoustikov, A., Sibley, S., Thompson, M. E. & Forrest, S. R. (1998) *Nature* 395, 151.
[4] D'Andrade, B., (2012) *Nature* 492, 197.
[5] Baldo, M. A., Lamansky, S., Burrous, P. E., Thompson, M. E. & Forrest, S. R. (1999) *Appl. Phys. Lett.* 75, 4.
[6] Lamansky, S., Djurovich, P., Murphy, D., Abdel-Razzaq, F., Kwong, R., Tsyba, I., Bortz, M., Mui, M., Bau, R. & Thompson, M. E. (2001) *Inorg. Chem.* 40, 1704.
[7] Duan, J. P., Sun, P. -P. & Cheng, C. -H. (2003) *Adv. Mater.* 15, 224.
[8] Beeby, A., Bettington, S., Samuel, I. D. W. & Wang, Z. (2003) *J. Mater. Chem.* 13, 80.
[9] DeRosa, M. C., Mosher, P. J., Yap, G. P. A., Focsaneanu, K. -S., Crutchley, R. J. & Evans, C. E. B. (2003) *Inorg. Chem.* 42, 4864.
[10] Ostrowski, J. C., Robinson, M. R., Heeger, A. J. & Bazan, G. C. (2002) *Chem. Commun.* 7, 784.
[11] Giridhar, T., Saravanan, C., Cho, W., Park, Y. G., Lee, J. Y. & Jin, S. -H. (2014) *Chem. Commun.* 50, 4000.
[12] Park, Y. H. & Kim, Y. S., (2007) *Thin Solid Films* 515, 5084.
[13] Sree, V. G., Cho, W., Shin, S., Lee, T., Gal, Y. -S., Song, M. & Jin, S. -H. (2017) *Dyes and Pigments* 139, 779.

[14] Zhen, C. -G., Dai, Y. -F., Zeng, W. -J., Ma, Z., Chen, Z. -K. & Kieffer, J. (2011) *Adv. Funct. Mater.* 21, 699.
[15] Park, J., Park, J. S., Park, Y. G., Lee, J. Y., Kang, J. W., Liu, J., Dai, L. & Jin, S. -H. (2013) *Org. Electron.* 4, 113.
[16] Lee, S. -J., Park, J. -S., Song, M., Shin, I. A., Kim, Y. -I., Lee, J. W., Kang, J. -W., Gal, Y. -S., Kang, S., Lee, J. Y., Jung, S. -H., Kim, H. -S., Chae, M. -Y. & Jin, S. -H. (2009) *Adv. Funct. Mater.* 19, 2205.